A DYNAMIC, COUPLED THERMAL RESERVOIR APPROACH TO ATMOSPHERIC ENERGY TRANSFER PART I: CONCEPTS

Roy Clark, Ph.D.
Ventura Photonics
1336 N. Moorpark Road #224
Thousand Oaks, CA 91360 USA

ABSTRACT

A dynamic, coupled thermal reservoir description of the Earth's atmospheric energy transfer processes is presented. Solar heat is stored and released by four coupled reservoirs, the land, the oceans and the upper and lower troposphere. In addition to the temperature, there are three other important parameters need to be considered. The first is the thermal gradient, the second is the interaction length and the third is the time delay or phase shift between the incident flux and reservoir thermal response. The Earth's climate is stabilized by the heat stored in these thermal reservoirs, particularly the oceans and the lower troposphere up to 2 km. Almost all of the downward LWIR flux reaching the surface originates in the lower troposphere. The dominant energy transfer process within the troposphere is moist convection. At night, the lower troposphere acts as a thermal blanket that slows the surface cooling. The upper troposphere cools continuously by LWIR emission to space. A change in temperature requires a change in the heat stored in the reservoir that has to be calculated using the heat capacity and the time dependent flux balance. The long wave infrared (LWIR) flux cannot be separated and used to define a change in 'average surface temperature' using blackbody theory.

Keywords: Carbon Dioxide, Dynamic Coupled Thermal Reservoirs, Greenhouse Effect, Interaction Length, Meteorological Surface Air Temperature, Ocean Warming, Phase Shift, Radiative Transfer, Thermal Storage, Urban Heat Island Effect.

1. INTRODUCTION

Fourier described the thermal storage properties of the Earth in 1827.[1] He recognized that diurnal and seasonal solar heating penetrated to different surface depths and that there was a time delay or phase shift between the incident surface flux and the subsurface temperature changes. He also understood the role of atmospheric convection in thermal transport from the surface. The concept of an Ice Age was introduced by Agassiz in 1837.[2,3] However, the explanation, in terms of Milankovitch cycles was not published for almost another century.[4,5] In the mean time, speculation that climate change could be caused by variations in the atmospheric concentration of CO_2 started to become the accepted scientific dogma.[6] The CO_2 monitoring station on Mauna

Kea was established by Keeling in 1958.[7] Soon after, the availability of computers enabled more complex atmospheric radiative transfer calculations to be performed. However, climate change predictions were still based on very simple models. Early modeling assumptions were clearly described by Manabe and Wetherald in 1967.[8] They included an exact 'equilibrium' flux balance between an 'average' incident solar flux and an 'average' outgoing LWIR flux. Furthermore, the Earth's surface was treated a black body surface with zero heat capacity. These assumptions lead to a very simple 'radiative forcing' model in which the effect of changes in atmospheric CO_2 concentration can be analyzed by applying perturbation theory to a set of coupled flux equations.[9] This approach led to a major advance in atmospheric radiative transfer computation. Unfortunately the results have little or no application to a real climate in which time varying solar, LWIR and convective fluxes are coupled to thermal reservoirs with large heat capacities. In order to model such a dynamic climate system, we have to return to the basic heat transfer concepts that were originally described by Fourier two centuries ago. The surface temperature is determined by the time dependent flux balance of a series of coupled reservoirs. However, in addition to the temperature, there are three other important parameters need to be considered. The first is the thermal gradient, the second is the interaction length (depth or path length) and the third is the time delay or phase shift between the incident flux and reservoir thermal response.

The Earth's climate is stabilized by ocean thermal storage and long range ocean thermal transport. The oceans are cooled at the surface by a combination of wind driven evaporation and LWIR emission. These processes only couple to the first 100 micron layer of the ocean.[10-12] Below this, within the first 100 m depth, ocean temperatures are determined by the balance between solar heating and the downward transport of cooler water from the surface.[13,14] The interaction of the wind speed with the ocean thermal reservoir induces long term thermal fluctuations in the ocean surface temperatures that produce characteristic quasi-periodic ocean thermal oscillations including the El Nino Southern Oscillation (ENSO), the Pacific Decadal Oscillation (PDO) and the Atlantic Multi-decadal Oscillation (AMO).[15-17] Long term climate change is caused by small variations in the solar flux that accumulate in the oceans. The average incident solar flux at the top of the atmosphere is approximately 1365 ±1 W m^{-2}.[18] This may be used to assign an approximate climate change budget. The change from 0 to +1 W m^{-2} may be attributed to variations in the solar flux as determined from the sunspot cycle or other indicators of the solar flux intensity such as ^{10}Be and ^{14}C isotope ratios.[19] The change from 0 to -1 W m^{-2} may be attributed to changes in the ellipticity of the Earth's orbit.[4,5] The variations in the solar flux have produced the Medieval Warming Period, the Maunder Minimum or Little Ice Age (LIA) and the recent Modern Maximum.[20] Variations in the Earth's orbital ellipticity have produced the recent 100,000 year Ice Age cycles.[21-23] Small changes in solar flux can accumulate in the ocean reservoir gyre system because the penetration depth can reach 100 m. The penetration depth of the LWIR flux is limited to the thin surface cooling layer.

This work is the continuation of research described in a previous paper 'A Null Hypothesis for CO_2' that was published as part of the 2010 E&E Special Issue 'Paradigms in Climate Research'.[14,24] The conclusion to this earlier paper was that ***'It is impossible to show that changes in CO_2 concentration have caused any change to the Earth's climate, at least since the current composition of the atmosphere was set by ocean photosynthesis about one billion years ago'***. This was based on the results of a combination of thermal reservoir modeling of land and ocean heating and a high resolution radiative transfer analysis of the atmospheric cooling flux that included molecular line narrowing effects. Since then, a more detailed analysis of land and ocean heating and atmospheric heat transfer has been performed, based on a combination of measured flux and weather station data and high resolution radiative transfer calculations. This work is presented here in two parts. In Part I, in this paper, the basic concepts of time dependent coupled thermal reservoirs are considered. In particular, it is shown that the troposphere divides naturally into two separate thermal reservoirs. The lower tropospheric reservoir acts as a 'thermal blanket' that slows the night time cooling and maintains the surface temperature. The radiative cooling to space occurs mainly from the upper tropospheric reservoir. The coupling of the heat from the surface to the tropospheric reservoirs is through moist convection. At the surface, the air-land and air-ocean interfaces have significantly different energy transfer properties. This leads to a basic description of the atmospheric energy transfer in terms of four coupled thermal reservoirs, the oceans, the land and the lower and upper thermal reservoirs. The so called 'greenhouse effect' is explained in terms of daytime convective heating and night time thermal storage within the lower tropospheric reservoir. There is no 'average equilibrium surface temperature' that is controlled by an 'average' flux balance. In Part II in the following paper, the application of the concept of coupled thermal reservoirs is applied to selected meteorological data. In particular, the effects of thermal storage, wind driven evaporation and the diurnal convection cycle on the reservoir coupling are examined. The observed dependence of meteorological station data on ocean surface temperatures is also investigated. In all cases, the effects of a 100 ppm increase in the atmospheric concentration of CO_2 on the reservoir thermal properties are too small to be measured.

2. THE LAND AND OCEAN THERMAL RESERVOIRS AND THE AIR-LAND AND AIR-OCEAN INTERFACES

The sun heats the land and ocean thermal reservoirs during the day. Over land, the solar flux is absorbed and converted into heat at the surface. Thermal storage effects are localized and limited to a few meters in depth. Over the oceans, almost all of the solar flux is transmitted below the ocean surface. The amount of heat that is stored in these reservoirs is determined by the cumulative effect of the short term time dependent flux balance at the surface. The solar heating establishes a set of time dependent thermal gradients that cool the surface through a combination of moist convection and net LWIR emission. These processes couple the surface heat back into the atmosphere. In addition, over land, the increase in surface temperature creates

a thermal gradient that conducts heat down into the subsurface layers. This heat is released later in the day as the surface cools. Under full summer sun conditions, the dry land surface temperature may reach or exceed 323 K (50 C). Over the oceans, the temperature rise is much smaller, typically near 2 K. The solar heating is distributed over a range of ocean depths. The dominant surface cooling process is the wind driven surface evaporation. The water in the cooler surface 'skin layer' sinks and cools the warmer water below. In addition, the heat stored in subsurface ocean layers can be transported over very long distances by wind driven ocean currents.

All of the surface cooling flux that heats the atmosphere is coupled directly or indirectly through convection. The convective or sensible heat flux is produced by the direct heating of the air at the surface. Evaporation adds water vapor to the convective flux and cools the surface through the loss of latent heat. The latent heat flux is normally treated as a separate flux term. As the warm air rises it cools. This establishes the local lapse rate or vertical atmospheric temperature profile.[25] Water condenses and forms clouds above the saturation level. This releases latent heat which produces additional convection. The convection process involves a complex turbulent eddy current flow pattern that mixes the warm air with the surrounding cooler air. The upward blackbody flux from the surface is partially balanced by the downward LWIR flux from the atmosphere. The net surface LWIR flux is divided between two separate energy transfer paths. Within the atmospheric LWIR transmission window, the LWIR flux is transmitted directly to space. However, outside of this window within the atmospheric absorption bands, any net excess LWIR flux is absorbed and converted to heat that adds to the convective flux. In addition to the net surface flux absorption, direct absorption of the incoming solar flux in the IR and NIR spectral regions by H_2O and CO_2 also adds to the atmospheric convection. After sunset, the air-land surface interface cools until the surface and air temperatures are approximately equal. Almost all of the heat stored below the surface is released and convection effectively stops. Surface cooling is now limited to the net LWIR flux emitted through the LWIR atmospheric transmission window. This slows the surface cooling and maintains the surface temperature at night. Advection also contributes to the atmospheric thermal energy transport, particularly at higher altitudes. The basic reservoir energy transfer processes are illustrated in Figure 1.

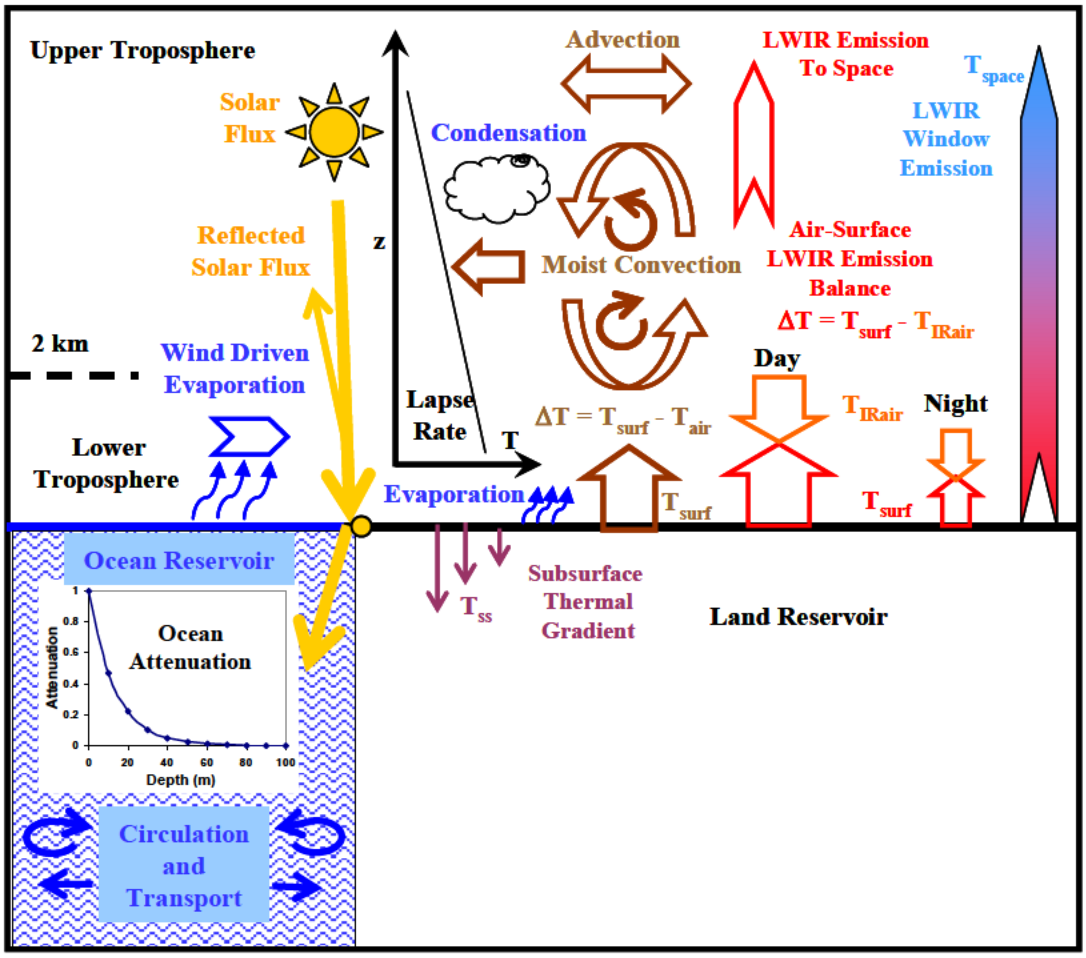

Figure 1: Dynamic energy transfer (schematic). The sun only heats the thermal reservoirs during the day. Over land, the solar heating is localized. Atmospheric heating is by moist convection which sets the lapse rate. At night, convection almost stops and the lower troposphere cools slowly by LWIR emission. In the oceans, the solar flux can penetrate to 100 m depth. The ocean can only cool at the surface and the dominant cooling process is wind driven evaporation. See text for further details.

At the air-land or air-ocean interfaces, a basic heat transfer flux balance for a time interval Δt may be written as:[26]

$$C_s \Delta T x = \Delta Q_{sun} - \Delta Q_{irnet} - \Delta Q_{sens} - \Delta Q_{lat} - \Delta Q_{ssc} \quad (1)$$

where C_s is the heat capacity of the surface layer, T is the surface layer temperature and x is the layer thickness, Q_{sun} is the absorbed solar flux, Q_{irnet} is the net LWIR cooling flux, Q_{sens} is the sensible heat flux or dry air convection, Q_{lat} is the latent heat flux and Q_{ssc} is the subsurface heat transport. The time interval is typically 0.5 to 2 hours, based on short term meteorological station data averages. Long term climate change is determined by the overall trend in the short term data.

The incident solar flux may be determined using a polynomial expansion of the solar elevation angle θ_e.[26]

$$\Delta Q_{sun} = a_{surf}(A + B\theta_e + C\theta_e^2 + D\theta_e^3 \ldots\ldots) \quad (2)$$

θ_e is calculated from the hour angle, h, the solar declination δ and the local latitude ϕ.

$$\sin\theta_e = \cos h\cos\delta\cos\phi + \sin\delta\sin\phi \quad (3)$$

The fraction of the solar flux absorbed at the surface, a_{surf} depends on the angle of incidence and the surface material absorbance. The solar flux term provides the initial diurnal and seasonal time dependence of the flux balance. The heating of the air-land and air ocean thermal reservoir interfaces produces the thermal gradients needed to dissipate the solar flux as heat. The penetration depth and phase shift depend on the detailed thermal and spectroscopic properties of the surface materials.

The surface black body LWIR emission is given by Stefan's Law. The downward LWIR flux from the atmosphere should be calculated using radiative transfer theory. However, this may be simplified for discussion purposes by using Stefan's Law modified with a fixed atmospheric spectral window.[26] The net LWIR flux then becomes:

$$\Delta Q_{irnet} = \sigma(T_s^4 - T_a^4) + \Delta Q_{irwin} \quad (4)$$

Here, σ is Stefan's constant, T_s is the surface temperature, T_a is the surface air temperature and ΔQ_{irwin} is the LWIR transmission window loss. The spectral window can be set for example to 900 to 1100 cm^{-1}, which gives a window transmission flux of approximately 50 W m^{-2} at 288 K (15 C). Eqn. (4) provides a simple illustration of a complex LWIR flux balance process. Figure 9 in Part II gives a plot of measured net LWIR flux data for the 'Grasslands' site that shows the effects of humidity and cloud cover.[13]

Convection is a complex turbulent mixing process. The convective surface cooling or sensible heat flux is often simplified by using a single convection coefficient k_{conv} and the bulk surface–air temperature difference.

$$\Delta Q_{sens} = k_{conv}(T_s - T_a) \quad (5)$$

Over dry land, k_{conv} is approximately 15 to 20 W m^{-2} K^{-1}.[13] Over the oceans it is near 5 W m^{-2} K^{-1}.[27]

The surface is also cooled by water evaporation that is coupled to the convective flux. This reduces the dry surface temperature rise. Over water, the latent heat flux depends on the water surface concentration gradient and the wind speed.[28-30] Over land, the description of the surface evaporation (evapotranspiration) is complex.[31] The latent heat flux usually peaks during the middle of the day and decreases significantly at night. However, the flux may also be limited by the transport of subsurface moisture to the surface. The ocean latent heat flux can be calculated using.[28]

$$\Delta Q_{lat} = k_{lat}(P_{Tws} - R_h P_{Twa})U \quad (6)$$

Here, k_{lat} is an empirical convection coefficient, P_{Tws} is the saturated water vapor concentration at the surface temperature T_s, P_{Twa} is the saturated water vapor concentration at the surface air temperature T_a, R_h is the relative humidity and U is the wind speed.

Over land, the subsurface heat transfer process is conduction, which depends on the subsurface thermal gradient, the subsurface depth, x, and the thermal conductivity, k_{cnd}.

$$\Delta Q_{ssc} = k_{cnd}(T_s - T_{ss})/x \quad (7)$$

The thermal conductivity may be calculated analytically using a finite element approach.[32] Over the ocean, almost all of the solar flux is transmitted through the ocean surface. Ocean heating has to be calculated using a combination of depth dependent solar absorption and downward layer mixing or diffusion.[13] The absorption of sunlight by water is given below in **Error! Reference source not found.**. Ocean heating in the Pacific warm pool is considered in Part II.

Under full summer sun conditions, the solar flux reaching the surface of the Earth is approximately 25 MJ m^{-2} day^{-1}. The peak solar flux during the middle of the day is near 1000 W m^{-2}, or 3.6 MJ m^{-2} hr^{-1}. At night the solar flux is zero. Over land, almost all of this flux is dissipated back into the atmosphere on the day that it is received. The Second Law of Thermodynamics requires that the heat flow follows the thermal gradient. However, there is no requirement that the heating and cooling flux exactly balance on any time scale. The First Law of Thermodynamics only requires conservation of energy, not conservation of flux. The heat can

be stored and released later. There are at least five time dependent thermal gradients that operate to dissipate the solar flux. These are:

$$\Delta T_1 = T_{swin} \quad (8a)$$

$$\Delta T_2 = T_s - T_a \quad (8b)$$

$$\Delta T_3 = T_s - T_{aeff} \quad (8c)$$

$$\Delta T_4 = T_L(z) \quad (8d)$$

$$\Delta T_5 = T_s - T_{ss} \quad (8e)$$

ΔT_1 is the temperature difference between the surface and outer space that defines the LWIR transmission window. Typically, this would just be the surface temperature, T_s. ΔT_2 is the bulk surface air temperature difference that determines the surface convection or sensible heat in Eqn (5). It also determines the saturated water vapor pressure difference in Eqn (6). ΔT_3 is the surface air temperature difference used to determine the net LWIR flux in Eqn (4). ΔT_4 is the lapse rate. In conjunction with the humidity, this determines that atmospheric temperature and species profile that in turn defines the downward LWIR flux at the surface. It also contributes to the convective buoyancy or rate of ascent of the air convection from the surface. ΔT_5 is the subsurface thermal gradient.

There are three important points to note about the thermal gradients. First, for a dry land surface, as the surface–air temperature difference increases, the sensible heat flux increases faster than the net LWIR flux. Second, atmospheric absorption converts most of the net surface LWIR flux to additional convection. Third, the ocean latent heat flux is dependent on both the temperature/humidity difference and the wind speed.[27-30] Figure 2 illustrates the diurnal flux balance for dry convection over land under full summer sun conditions. This is derived from the Ameriflux 'Grasslands' data set described in Part II.[33] The solar heating flux, the convection and net IR cooling fluxes and the subsurface thermal transfer are plotted for a 24 hour cycle in Figure 2a. The corresponding surface and air temperatures are shown in Figure 2b. The total thermal flux dissipated by the surface during the 24 hour period from both net LWIR emission and convection in Figure 2a is 25.4 MJ m^{-2} representing full summer sun 'clear sky' conditions. Of this, approximately 23 MJ m^{-2}, or 90% is dissipated during the day and early evening. The convective flux is 14.5 MJ m^{-2}or 57% of the total flux and the associated LWIR flux is 8.5 MJ m^{-2} or 33% of the total flux. Only 2.4 MJ m^{-2} is dissipated at night through the LWIR transmission window. The time delay or phase shift between the maximum solar flux and surface cooling flux in this case is almost 2 hours. Convection continues after sunset until the ground and air temperatures equalize. After that the surface cooling is limited to the net LWIR flux. The lower tropospheric reservoir now acts as a 'thermal blanket' that slows the night time cooling. This is how the surface temperature is maintained at night. The lower troposphere also cools slowly by

LWIR emission. This can be seen in Figures 5 through 7 below. However, most of the LWIR cooling flux is emitted at higher altitudes. The night time surface cooling flux typically varies between 0 and 100 W m^{-2}, depending on humidity and cloud cover. This is shown in Figure 9 in Part II for the Ameriflux 'Grasslands' data set. Thermal storage effects in the lower troposphere are further illustrated in Part II, Figures 13 and 14 using radiosonde data from the San Diego Miramar Station. This is the nearest radiosonde station to the 'Grasslands' site.

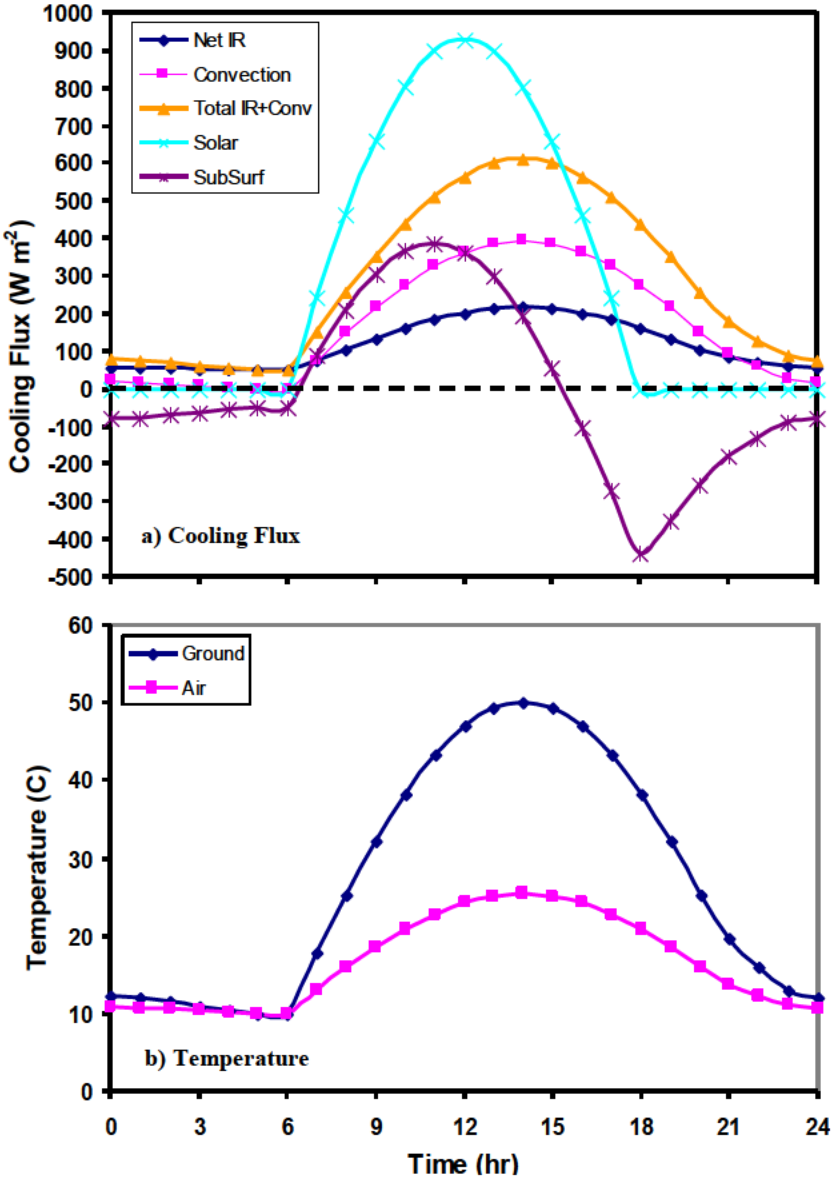

Figure 2: Diurnal surface and air temperatures and the dry convection surface flux terms for full summer sun illumination conditions. The surface temperature in b) is determined by the dynamic flux balance of the terms in a). The air temperature rise in b) is produced by convective heating from the surface.

The observed 100 ppm increase in atmospheric CO_2 concentration has produced an increase in the downward atmospheric LWIR flux at the surface increase of approximately 1.5 W m^{-2}.[14] This is too small to have any measureable effect on surface temperatures when it is added to the net LWIR flux term and used to calculate the total flux balance. This follows from Eqn. (1) when the time dependent flux terms are modified to include the small additional net IR flux term. For example, as shown in Part II, Figure 11 using a simple surface flux model based on the Ameriflux data set, a maximum increase in surface temperature of 0.067 C was obtained when 1.5 W.m^{-2} was added to the LWIR flux. The surface temperature is determined by the heat stored dynamically in the surface layer. The heat transfer at the land-air interface is limited to a thin surface layer less than 1 mm thick, but this is coupled by conduction to the subsurface below. As the heat flux through the surface layer changes, so do the temperatures that determine the thermal gradient. The additional 1.5 W.m^{-2} in LWIR flux is too small to cause a measurable change in the thermal gradient. The temperature is determined by the Second Law of Thermodynamics, not the First.

Over the oceans, almost all of the incident solar flux is transmitted through the surface. At least half of this flux is absorbed in the first meter layer. The oceans cool at the surface through a combination of net LWIR emission and moist convection. The dominant process is wind driven evaporation. In this case, the increase of 1.5 W.m^{-2} in the net LWIR flux is too small to cause a measurable change in the surface evaporation. The total daily increase in flux from 1.5 W.m^{-2} is 0.13 MJ m^{-2} day^{-1}. This is equivalent to approximately 2.2 minutes of full summer solar flux or the evaporation of a surface layer of water with an area of 1 m^2 and a thickness of 54 μm. In the Pacific Warm Pool, from Figure 5 of Part II, this volume of water can be evaporated by a change in average daily wind speed of approximately 0.04 m s^{-1}.

3. THE LOWER AND UPPER TROPOSPHERIC THERMAL RESERVOIRS

As discussed above, the troposphere splits naturally into two independent thermal reservoirs based on their energy transfer properties.[13] The lower thermal reservoir extends up to an altitude of approximately 2 km. Almost all of the LWIR flux reaching the surface from the atmosphere originates from within this reservoir. It is heated during the day by convection and cools slowly at night by LWIR emission. The surface acts as ‘heat pump’ that removes heat from the air at the base of this reservoir by net LWIR emission mainly through the LWIR transmission window. This reservoir also cools through LWIR emission at the interface between the upper and lower tropospheric reservoirs. However, unlike the land and ocean surfaces, this interface is not a distinct boundary. It is the approximate altitude where the downward LWIR emission no longer has any significant influence on the surface flux balance.

The upper tropospheric reservoir extends from 2 km up to the tropopause. It cools continuously by LWIR emission to space and is heated during the day by moist convection from below. The height of the tropopause varies with latitude and season. Over the tropics, when convection is driven by strong tropical thunderstorm activity, it may extend up to 18 km.[34] At high latitudes, the tropopause height is typically near 8 km. The US standard atmosphere sets the tropopause near 11 km with an average lapse rate of -6.5 K km^{-1}.[35] The corresponding tropopause temperature is 216.5 K (–56.5 C) and the pressure is near 0.2 atm. The maximum LWIR cooling emission in the upper tropospheric reservoir occurs from water vapor in a limited altitude band with temperatures in the 240 to 260 K range. This emission band shifts in altitude as the surface temperature and the height of the tropopause change. This is illustrated in Figure 6 below.

The detailed description of the high resolution atmospheric radiative transfer calculations is complex and only a brief overview and summary of the pertinent results will be presented here. The results are derived from high resolution radiative transfer calculations using a spectral resolution of 0.01 cm^{-1} and an altitude resolution of 100 m. Further details are given in.[14]

Within the atmospheric absorption bands, LWIR radiation is absorbed and emitted. For a given gas volume, the IR active molecules absorb part of the upward LWIR flux from below and the downward LWIR flux from above. In addition, they emit LWIR radiation equally in both the upward and downward directions. The absorption and emission properties depend on the IR species concentration, the temperature, the pressure and the molecular line profile. The temperature of the IR active molecules is the same as the local bulk air temperature. The net heating or cooling depends on the balance between the absorption and emission terms. The molecular collision frequency in troposphere is larger than 10^9. This means that as soon as an IR photon is absorbed, the excited molecular vibration-rotation state is quenched by collisions and the thermal energy transferred to the local air mass. Conversely, the emission of IR photons removes heat from the local air mass. This means that the LWIR flux is always coupled to the bulk thermal mass of the air in the atmosphere.

The IR absorption bands in the atmosphere consist of thousands of overlapping lines. Historically, detailed line by line radiative transfer calculations were difficult and time consuming. Instead, simplified band models were used to approximate the LWIR flux. These gave reasonable results for the total flux at the top and bottom of the atmosphere, but the lineshape dependence was lost.[36] Today, the high resolution line by line computation of the LWIR flux is relatively straightforward. The required spectral parameters are available from the HITRAN database.[37] This database has been compiled over many years by various research groups operating independently of climate science. Once the atmospheric temperature and species profile is defined, the atmospheric LWIR flux may be reliably determined using the

HITRAN data. The spectral units that used in HITRAN are wavenumbers, ν cm^{-1}. This is the reciprocal of the wavelength in cm.

For a given wavenumber, ν, the single line absorption is given by

$$I = I_0 \exp[-L(\nu,p) S_{\nu 0T} C_M x] \quad (9)$$

Where I_0 is the incident light intensity, $L(\nu,p)$ is the pressure dependent Lorentzian line profile, $S_{\nu 0T}$ is line strength at the atmospheric profile temperature T, C_M is the molecular species concentration and x is the path length. The total atmospheric absorption is the sum of all of the molecular line contributions to each spectral interval. Further details of the HITRAN calculations are given in reference [**37**]. The important point is that the attenuation and the molecular linewidths decrease as the pressure, temperature and the species concentration decrease with altitude. In particular, the water vapor concentration decreases rapidly as the temperature decreases and the water condenses. The radiative transfer process of absorption and emission is gradually replaced by a transition to a free photon flux. This is illustrated in Figure 3.

Figure 4 shows the cumulative downward LWIR flux reaching the surface for five different conditions of humidity, surface and air temperature. Over 90% of the downward LWIR flux originates from within the first 2 km layer. Similarly, over 90% of the upward LWIR flux from the surface is absorbed within this 2 km layer. The spectrally resolved absorption vs. altitude for a surface/air temperature of 325/295 K at 50% relative humidity is shown in Figure 5. For this case, 75% of the surface flux is absorbed within the first 100 m. Further details are given in references [13] and [14]. The upper limit to the local LWIR flux for a specific molecular line is the blackbody emission at the local air temperature within the same spectral range as the line. In this case, all of the incident LWIR flux is absorbed within a short interaction path length and replaced by LWIR emission from the local air volume.

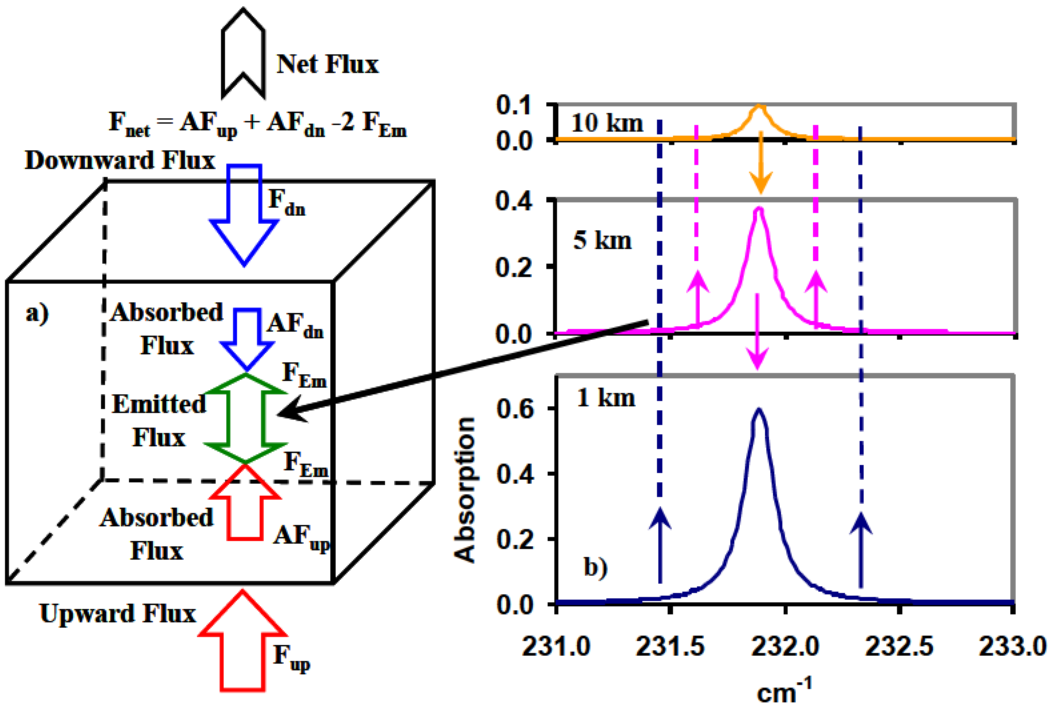

Figure 3: a) The atmospheric absorption and emission process and b) line narrowing effects.

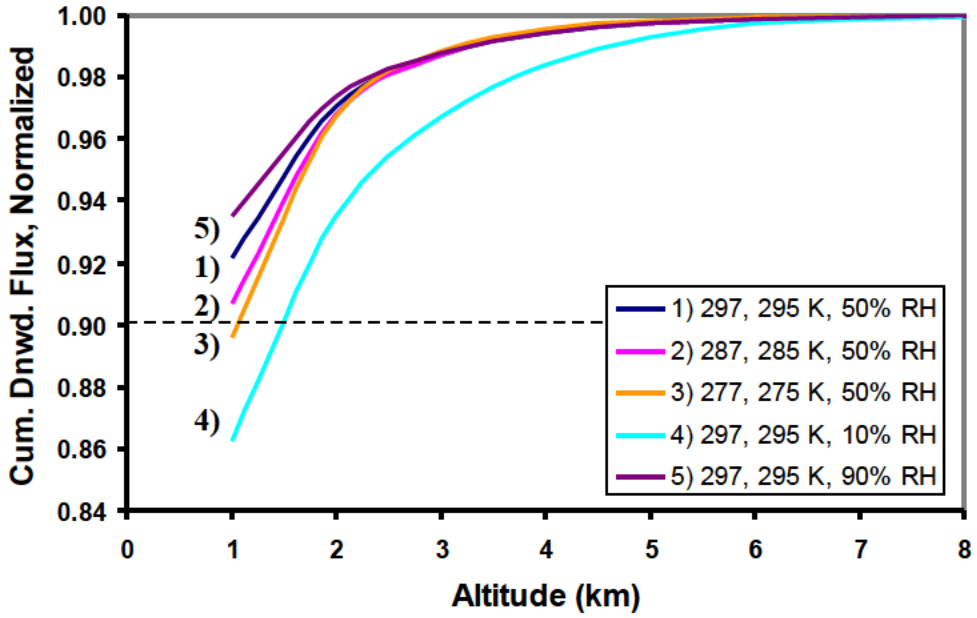

Figure 4: Cumulative normalized downward LWIR atmospheric flux vs. altitude, (total flux, 200 to 2000 cm^{-1}). Most of the downward LWIR flux originates from within the first 2 km air layer.

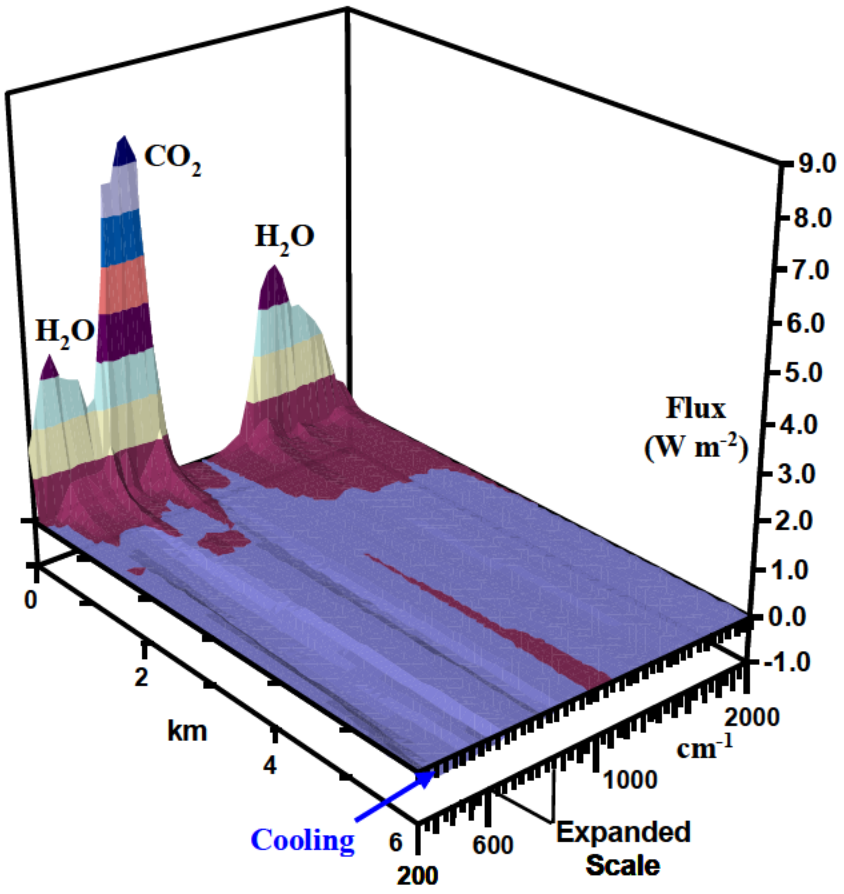

Figure 5: Spectrally resolved absorbed flux vs. altitude. Only the H_2O and CO_2 bands are shown. The surface temperature is 325 K, the surface air temperature is 295 K, and the RH is 50%. 75% of the LWIR radiation from the surface is absorbed in the first 100 m. (H_2O and CO_2 only - truncated data set, see [13] and [14] for further details).

The cooling of the upper thermal reservoir by LWIR emission is dominated by emission from the water bands.[38] Figure 6 shows a plot of the calculated net emission vs. altitude up to 9 km for surface/air temperatures of 297/295 K, 287/285 K and 277/275 K with 50% RH and 380 ppm CO_2. The 2 K surface-air temperature difference is representative of the ocean-air reservoir interface. The plot shows total net absorption in the 200 to 2000 cm^{-1} spectral range and the negative sign means that there is net emission to space and therefore cooling. The altitude resolution is 100 m. The emission (cooling) flux is for each 100 m layer. The cumulative sum of this flux is the upward LWIR emission to space. The approximate contributions of H_2O and CO_2 to the total emission are plotted separately. The H_2O contribution was estimated by adding the flux from the spectral regions 200 to 550 cm^{-1} and 1200 to 2000 cm^{-1}. The CO_2 contribution was estimated from the total flux in the spectral region from 550 to 800 cm^{-1}. This spectral region also includes some H_2O lines. There is a minor discontinuity ('spike') in the radiative transfer model output at the transition of the lapse rate from -6.5K km^{-1} to the saturated lapse rate. The H_2O absorption lines show a peak cooling rate of ~-1.5 W m^{-2}. This is the net upward

free photon LWIR emission from a 100 m layer. It produces a cooling rate of approximately 0.1 K per hour in the middle troposphere. The emission peak shifts to lower altitude as the surface/air temperatures decreases, but the emission profile is similar for all cases. This is because the peak emission comes from an emission band in the H_2O concentration range from 10^{16} to 10^{17} molecules cm^{-3}. The corresponding temperatures are 240 to 260 K. Since there is only a 2 K difference between the surface and air temperatures, the net emission to space starts close to the surface, above 100 m. From 1 to 9 km, the total cumulative H_2O cooling rate was over 2.5 times larger than that of CO_2 at all surface temperatures. Figure 7 shows the absorbed flux vs. altitude for a surface/air temperature of 325/295 K and RH of 90, 50 and 10 %. The large thermal gradient is representative of the air-land interface under full summer sun illumination. The emission peak increases from an altitude of approximately 6 km to 7 km as the RH increases. The saturation altitude for the 10% RH case is at 5 km. There is a net absorption at altitudes below 1 km because of the higher surface temperature compared to Figure 6.

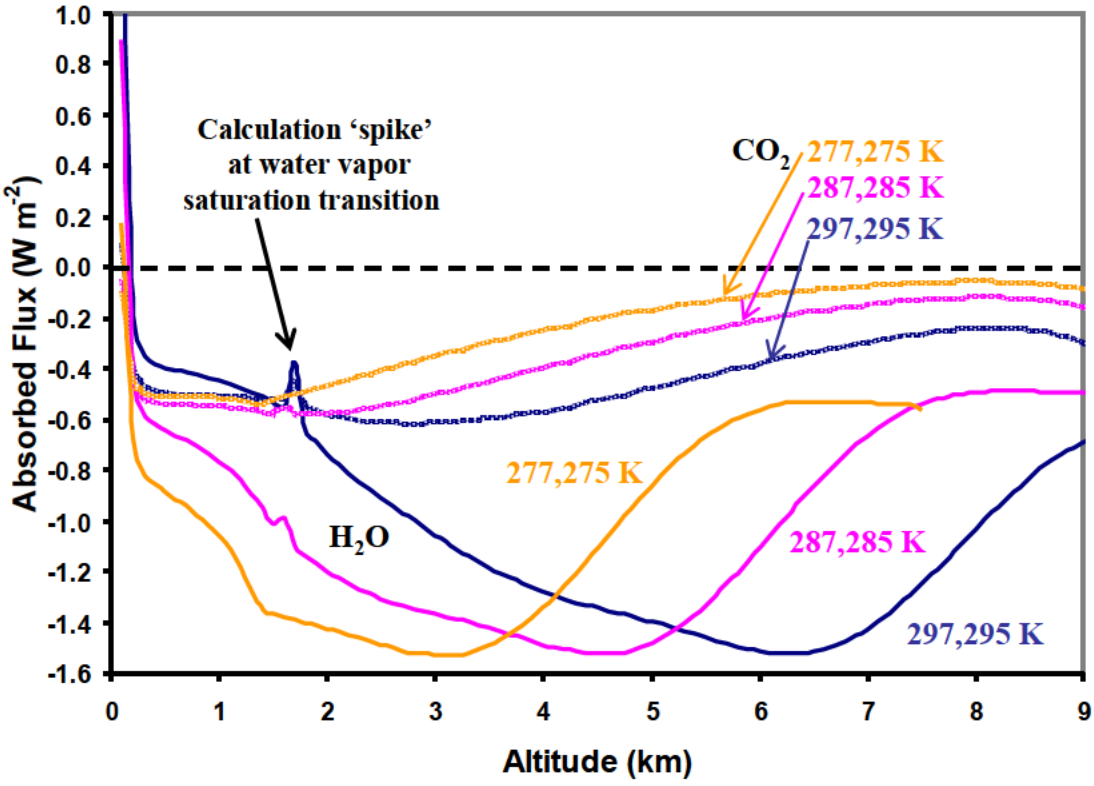

Figure 6: Absorbed flux vs. altitude for the surface/air temperatures of 297/295; 287/285 and 277/275 K, 50% RH, 380 ppm CO_2 and 100 m altitude resolution. The negative flux means that there is a net emission to space. The approximate contributions of H_2O and CO_2 to the total emission are shown separately (truncated data set, see [13] and [14] for further details).

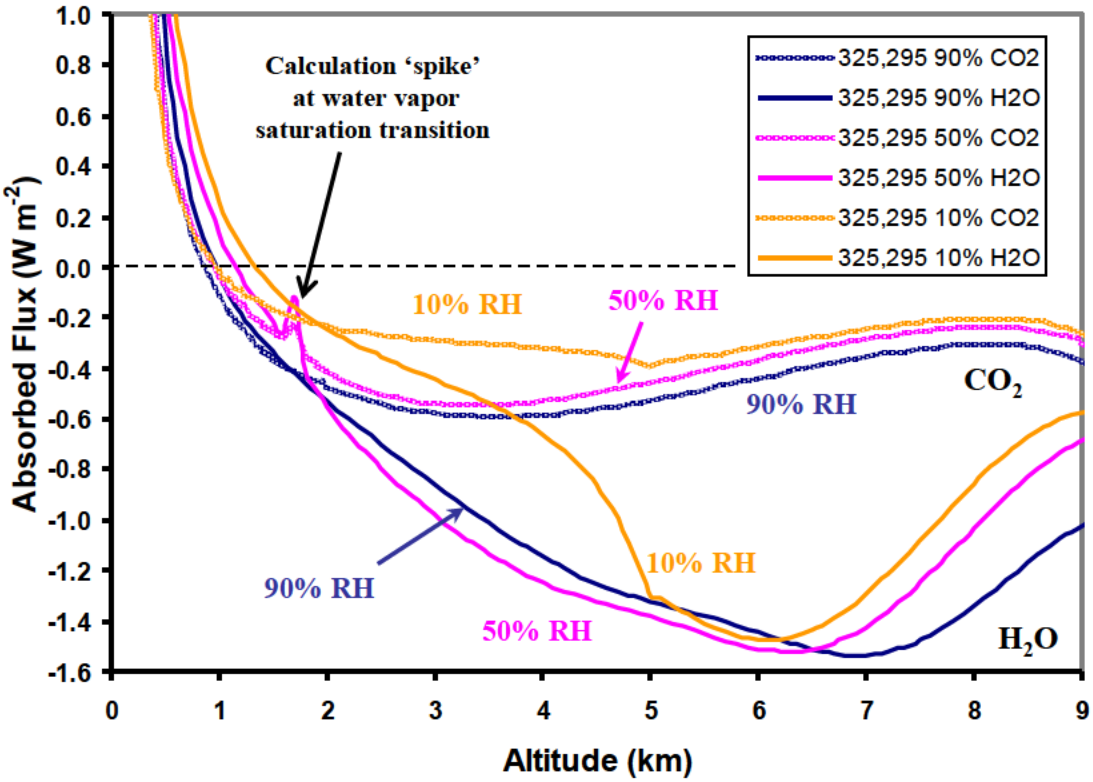

Figure 7: Absorbed flux vs. altitude for the surface/air temperature of 325/295 at 10, 50 and 90% RH, 380 ppm CO_2 and 100 m altitude resolution. The negative flux means that there is a net emission to space. The approximate contributions of H_2O and CO_2 to the total emission are shown separately (truncated data set, See [13] and [14] for further details).

Figures 3 to 7 clearly show that the upper and lower tropospheric thermal reservoirs are decoupled. The LWIR emission to space occurs mainly from the upper thermal reservoir and the downward LWIR flux reaching the surface comes from the lower surface reservoir. Both are heated by the convective flux that originates from the surface, the net LWIR absorption and latent heat release. The peak convective flux normally occurs in the afternoon, after the peak in the solar flux.[39] The sensible heat and almost all of the heating from the net atmospheric LWIR absorption are coupled to the lower thermal reservoir before reaching the upper reservoir. The release of latent heat depends on the local lapse rate, the humidity and the saturation level. There is no steady state or equilibrium flux. The LWIR emission to space continuously cools the upper tropospheric reservoir. It continues to cool through the night until it is warmed again by convection the following day. Both the convection and the LWIR flux are coupled to the same thermal reservoir and these energy transfer processes must be analyzed together for the coupled system.

The upward and downward LWIR fluxes are not equivalent because of the molecular line narrowing. The downward flux is emitted closer to line center and is absorbed by the broader

lines below. Upward LWIR emission from the wings of the broader lines at lower altitudes that is not reabsorbed becomes part of the free photon flux to space. This is illustrated above in Figure 3.

4. THE EFFECT OF A 100 PPM INCREASE IN ATMOSPHERIC CO_2 CONCENTRATION

Over the last 200 years, the atmospheric concentration of CO_2 has increased by 100 ppm from approximately 280 to 380 ppm. Since the start of continuous CO_2 monitoring by Keeling in 1958, the increase has been approximately 70 ppm.[7] Radiative transfer calculations show that the total increase in downward atmospheric LWIR flux at the surface from a 100 ppm increase in CO_2 concentration is approximately 1.5 W m^{-2}. The increase of 70 ppm since 1958 has contributed 1.2 W m^{-2} to this flux.[13,14,41] In order to assess the climate impact of this increase in LWIR flux it is also necessary to know the spectral distribution of the flux and how this couples to the thermal reservoirs, particularly the oceans. This is shown in Figure 8. The spectrally resolved downward LWIR flux is shown in Figure 8a for five CO_2 concentrations normalized to the 292 K black body surface emission with an air temperature of 290 K and an RH of 50%. The plots are low resolution summaries of high, 0.01 cm^{-1} resolution data. The increases in emission intensity in the P and R branches and in the overtones are indicated by the arrows. The attenuation depth for 99 % absorption into water is shown in Figure 8b.[40] The penetration depth of the LWIR flux from the P and R branches of CO_2 is less than 20 μm. The change in total downward LWIR emission intensity from Figure 8a is given in Figure 9. The calculated values are in good agreement with the 'radiative forcing constants' given by Hansen [**41**]. These are also plotted in Figure 9.[13,14]

However, Hansen [**41**] then uses the increase in downward LWIR flux to create an empirical 'radiative forcing constant' for CO_2 without any consideration of the surface energy transfer. Using the so called 'hockey stick' relationship between the climate temperature anomaly and the increase in atmospheric CO_2 concentration he derives the empirical relationship of 2/3 C increase in climate 'surface' temperature for each increase of 1 W m^{-2} in the downward LWIR flux from so called 'greenhouse gases'. This is based on the a-priori assumption that an increase in 'greenhouse gas' gas concentration must cause climate change. In order to evaluate the physical effects of the increase in atmospheric LWIR flux from CO_2 it is necessary use the coupled thermal reservoir approach given by Eqns (1-7). The increase in flux has to be added to the short term flux balance coupled to the reservoirs before any climate averaging is performed. When this is done, the effects of an increase in LWIR flux of 1.5 W m^{-2} are too small to measure. This is considered in more detail in Part II.

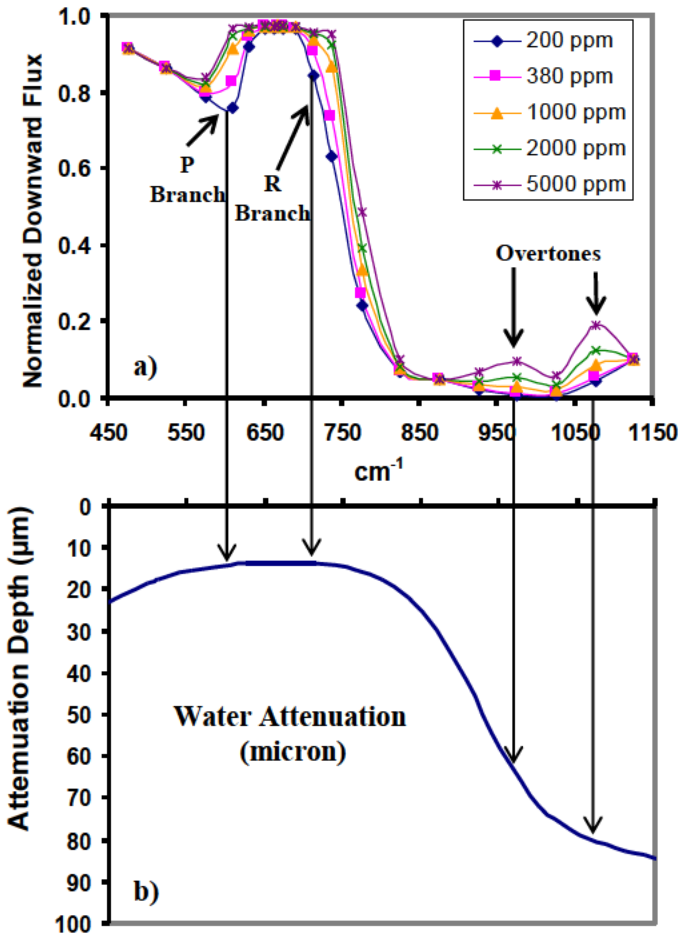

Figure 8: a) Spectrally resolved downward emission from CO_2 at the atmospheric concentrations indicated, 290 K air temperature, 292 K surface temperature, 50% RH. Spectra are normalized to the surface temperature emission. b) the water attenuation depth in micron for the CO_2 emission bands.

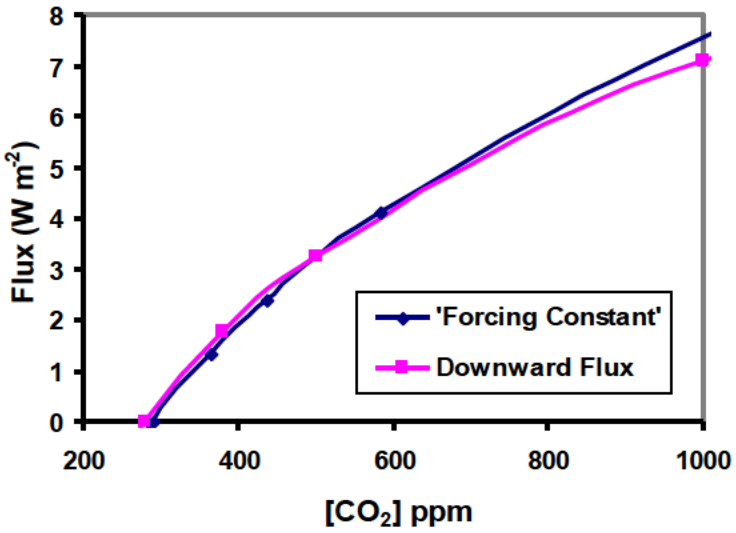

Figure 9: Change in total downward LWIR flux vs. CO_2 concentration from 300 to 1000 ppm.

The 1.5 W m^{-2} increase in the downward atmospheric LWIR flux from CO_2 at the surface originates from within the lower atmospheric reservoir. The radiative transfer properties of the upper atmospheric reservoir are also slightly changed. Figure 10 shows the effect on the absorption-emission profile of increasing the CO_2 concentration from 200 to 280, 380 and 500 ppm for surface/air temperatures of 325/295K, 297/295 K, 287/285 K and 277/275 K with the RH set to 50 %. The peak CO_2 emission occurs at altitudes between ~1 and 3 km. The magnitude of the peak emission is between -0.5 and -0.65 W m^{-2}. An increase of 100 ppm from 280 to 380 pp in CO_2 concentration decreases the peak cooling flux by approximately 0.017 W m^{-2}. For a 100 m column of air with a heat capacity of 1 kJ m^{-3} K^{-1}, this produces a decrease in the cooling rate of ~0.0006 K hr^{-1} or 0.015 K per day. For a total cooling flux of 2 W m^{-2}, the cooling rate for a 100 meter column of air is 0.07 K hr^{-1} or 1.7 K per day. A 100 ppm increase in atmospheric CO_2 concentration can have no measurable effect on the dynamic diurnal and seasonal energy balance that determines the tropospheric temperature profile.

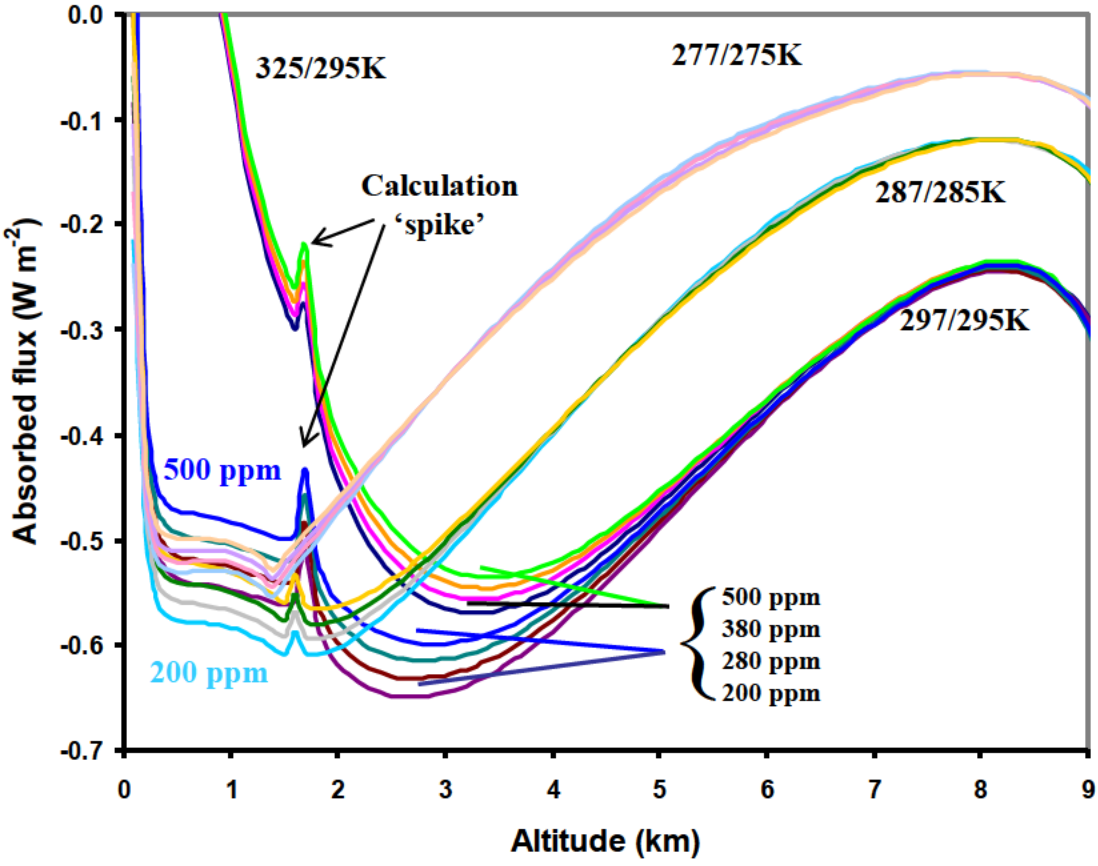

Fig **:e/air**
tem **The**
neg **cm^{-1}**
ran

5. CLIMATE INTERACTION LENGTHS AND TIMES: THE OCEAN-AIR INTERFACE

As shown above in Figure 8b, the interaction length of the CO_2 LWIR flux with the ocean surface is less than 100 micron. Surface evaporation is also limited to a similar interaction depth. Ocean cooling requires the downward transport of the cool surface layer into the warmer, solar heated layers below. There is both a diurnal and a seasonal mixing depth that depend on the balance between the solar heating and the downward mixing.[13,14] The ocean absorption of the solar flux from 300 to 2000 nm for near normal incidence is shown in Figure 11. Approximately half of the solar flux is absorbed within the first meter layer and 90% is absorbed within the first 10 meters.

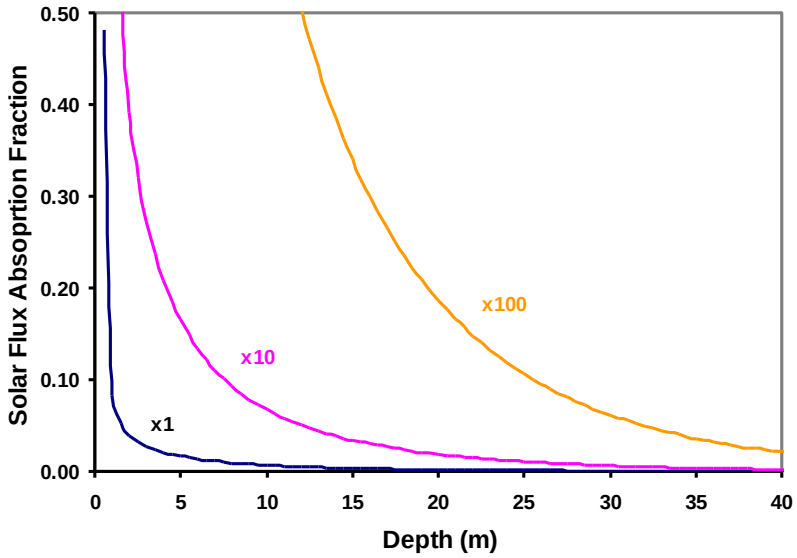

Figure 11: The absorption of the solar flux by water from 300 to 2000 nm.

The surface energy balance for the Pacific warm pool is illustrated schematically in Figure 12, based on Triton Buoy data. This is considered in more detail in Part II. The total daily solar flux coupled into the warm pool is approximately 22 MJ m^{-2} day^{-1}. Of this 11 MJ m^{-2} is absorbed in the first meter layer, 9 MJ m^{-2} in the next 9 m layer and the balance is absorbed at lower depths down to 100 m. The bulk surface ocean temperature is 30 C and this temperature extends down to 25 m. The air temperature is 29 C. The sensible heat flux is 5 W m^{-2} and the net IR flux is 50 W m^{-2}. At a wind speed of 5 m s^{-1}, the total net cooling flux just balances the absorbed solar flux. The latent heat flux is 195 W m^{-2}. However, from Eqn (6) the latent heat flux changes linearly with the wind speed. At a low wind speed, 1 m s^{-1}, the latent heat cooling flux decreases to 40 W m^{-2}. Under these conditions, the surface temperature starts to rise and so does the

sensible heat. This leads to the formation of tropical thunderstorms and increased surface cooling.[34] At high wind speed, the ocean gradually cools. The latent heat flux reaches 350 W m^{-2} at a wind speed of 9 m s^{-1}.

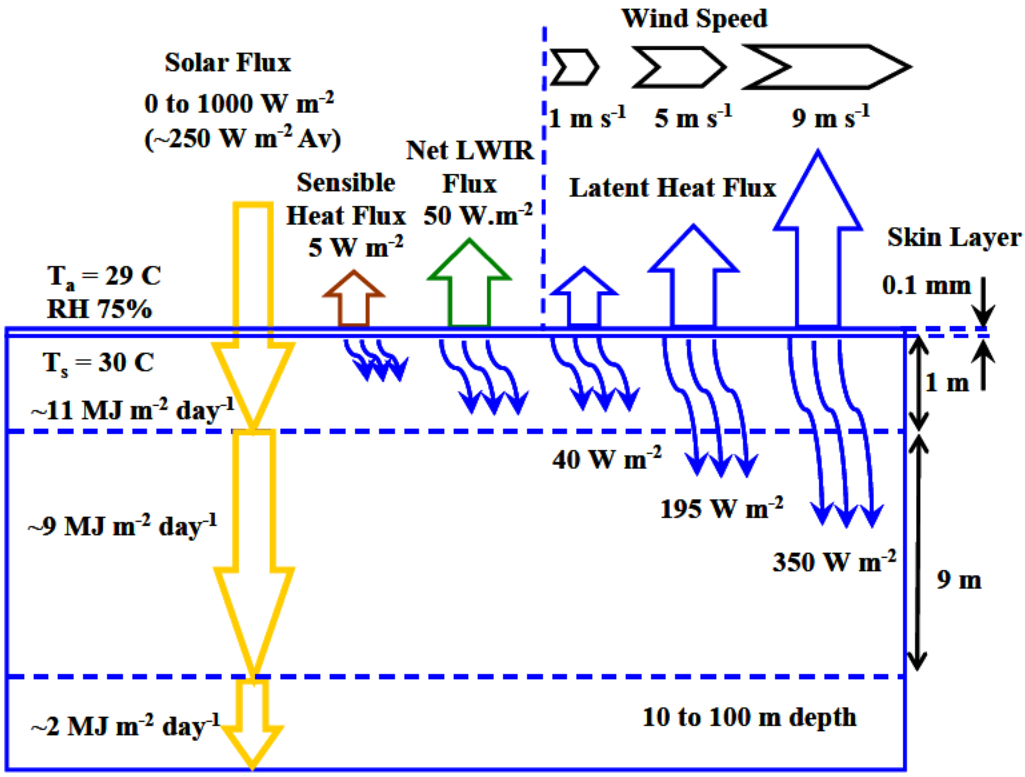

Figure 12: The ocean surface energy balance in the tropical warm pool. The evaporative surface cooling is strongly dependent on the wind speed.

The wind speed is an important consideration for ocean cooling, since it couples to the surface humidity gradient and drives the evaporation. It is also important because it determines the speed of the ocean currents. The surface mixing couples the wind driven surface momentum to the ocean current below. The entire ocean current down to depths of 100 m or more can move at the same velocity as the surface. The heating from the sun is fixed to a maximum of 25 MJ m^{-2} day^{-1}. However, the heating, for example of the ocean water in the equatorial Pacific depends on the interaction time, in this case the number of days required to transit the Pacific and reach the Pacific warm pool. This wind driven velocity-evaporation balance is the underlying mechanism that drives the ocean cycles. At higher latitudes, the surface area decreases because of the spherical geometry and the ocean currents are pushed to lower depths. This produces the so called re-emergence mechanism for long term ocean heat storage that also contributes to the ocean cycles.[42]

The upper and lower tropospheric thermal reservoirs are part of the general atmospheric circulation and are an integral component of the Earth's weather systems. Once a weather system is formed, it retains the bulk air temperatures associated with its formation. In order to change the air temperature, the entire air mass must be heated or cooled. Most weather systems are formed over the oceans. This means that ocean surface temperatures have a strong influence on climate. For example, the PDO and AMO cycles are a major factor in the continental US temperature record.[13,43] This is considered in more detail in Part II.

6. CONCLUSIONS

A dynamic, coupled thermal reservoir description of the Earth's atmospheric energy transfer processes has been presented. The atmospheric flux is coupled to a set of four thermal reservoirs, the land, the ocean and the lower and upper troposphere. A change in temperature requires a change in the heat stored in the reservoir determined using the heat capacity and the time dependent flux balance. The LWIR flux cannot be separated and used to define a change in 'average surface temperature' using blackbody equilibrium arguments. These concepts follow from the basic principles of heat transfer developed by Fourier over 200 years ago.[1] In addition to the temperature, there are three other important parameters need to be considered. The first is the thermal gradient, the second is the interaction length (depth or path length) and the third is the time delay or phase shift between the incident flux and reservoir thermal response.

The solar flux only heats the thermal reservoirs during the day. Thermal energy transfer through the air-land and air ocean interfaces to the atmosphere is therefore determined by a set of time dependent thermal gradients. All of the heat transferred from the surface to the atmosphere is coupled directly or indirectly through moist convection. In addition, the surface may cool by direct LWIR emission to space through the LWIR transmission window. A high resolution radiative transfer analysis of the LWIR flux shows that the troposphere divides naturally into two independent thermal reservoirs. The lower tropospheric reservoir extends from the surface to an altitude of approximately 2 km. The upper tropospheric reservoir extends from 2 km up to the tropopause. Almost all of the downward LWIR flux reaching the surface from the atmosphere originates from within the lower reservoir. This reservoir also absorbs almost all of the surface LWIR flux that is not transmitted through the LWIR window. Both tropospheric reservoirs are heated by convection, which normally peaks in the afternoon. At night, the lower troposphere acts as a thermal blanket that cools quite slowly by LWIR emission. This slows the night time cooling of the land and ocean reservoirs. The upper tropospheric reservoir cools continuously by LWIR emission to space. This process is determined by molecular line narrowing and the transition from radiative absorption emission to a free photon flux. The molecular line narrowing also means that the upward and downward LWIR fluxes are not equivalent.

The magnitude of the interaction lengths varies significantly. The LWIR flux and the latent heat flux are only coupled to the first 100 micron layer of the land and ocean reservoirs. Over land, thermal conduction limits the subsurface solar heating locally to a few meters. Over the oceans, the solar flux may penetrate to 100 meters depth. There is also a seasonal and a diurnal phase shift or time delay between the solar flux peak and the temperature response. The diurnal phase shift may delay the surface temperature peak by 2 hours. The seasonal phase shift may be 2 months. There can be no 'equilibrium flux balance'. This time dependent thermal reservoir description supersedes the conventional equilibrium absorption hypothesis of the greenhouse effect and the concept of radiative forcing. Over the last 200 years, the atmospheric concentration of CO_2 has increased by 100 ppm. This has produced an increase in the downward 'clear sky' atmospheric LWIR flux at the surface of 1.5 W m^{-2}. When this increase in LWIR flux is added to the time dependent short term flux balance coupled to the land and ocean thermal reservoirs, it has no measurable effect on surface temperature because of the large thermal heat capacities of the reservoirs and the large magnitudes and variations associated with the other flux terms.

7. ACKNOWLEDGEMENTS

This work was performed as independent research by the author. It was not supported by any grant awards and none of the work was conducted as a part of employment duties for any employer. The views expressed are those of the author. The author also acknowledges many helpful comments from other special section authors and anonymous referees.

REFERENCES

1. Fourier, B.J.B., Memoire sur les temperatures du globe terrestre et des espaces planetaires Mem. R. Sci. Inst. 1827, **7** 527-604

2. Agassiz, L., Etudes sur les Glaciers, Neuchatel, 1840.

3. Imbrie, J. and Imbrie, K.P., Ice Ages: Solving the Mystery, Harvard University Press, Cambridge, Mass. 1979.

4. Milankovitch, M, Théorie Mathématique des Phénomenes Thermiques Produits par la Radiation Solaire, Gauthier-Villars, Paris, 1920; Canon of Insolation and the Ice-Age Problem, Royal Serbian Acad. Sp. Pub. 132, 1941, Israel Program Sci. Trans, Jerusalem 1969.

5. Varadi, F., Runnegar, B. and Ghil, M., Successive refinements in long term integrations of planetary orbits, Astrophys. J., 2003, **562** 620-630.

6. Weart, S. R., The discovery of the risk of global warming, Physics Today 1997, **50**(1) 34-40.

7. Keeling curve data, 2012, http://scrippsco2.ucsd.edu/data/in_situ_co2/monthly_mlo.csv.

8. Manabe, S. and Wetherald, R. T., Thermal equilibrium of the atmosphere with a given distribution of relative humidity, 1967 J. Atmos. Sci., **24** 241-249.

9. Ramanathan, V. and Coakley, J.A., Climate modeling through radiative convective models Rev. Geophysics and Space Physics 1978, **16**(4)465-489

10. Gentemann, C.L., Wentz, F.J., Mears, C.A. and Smith, D.K., In situ validation of Tropical Rainfall Measuring Mission microwave sea surface temperatures, J. Geophys Res. 2004 **109** C04029 pp1-9.

11. Donlon, C. J.; Minnet, P.J., Gentemann, C. Nightingale, T.J., Barton, I.J., Ward, B. and Murray, M.J., 2002, Towards improved validation of satellite sea surface skin temperature measurements for climate research J. Climate 2002, **15** 353-369.

12. Zeng, X., Zhao, M., Dickinson, R.E. and He, Y., A multiyear hourly sea surface skin temperature data set derived from the TOGA TAO bulk temperature and wind speed over the tropical Pacific J. Geophys Res. 1999, **104** 1525-1536.

13. Clark, R., The dynamic greenhouse effect and the climate averaging paradox, Ventura Photonics Monograph, VPM 001, Thousand Oaks, CA, Amazon, 2011.

14. Clark, R., 'A null hypothesis for CO_2', Energy and Environment, 2010, **21**(4) 171-200.

15. Dijkstra, H. A., te Raa, L., Schmeits, M. and Gerrits, J., On the physics of the Atlantic multidecadal oscillation, Ocean Dynamics 2006, DOI 10.1007/s102360005-0043-0

16. Kao, H-Y. and Yu, J-Y., Contrasting Eastern-Pacific and Central-Pacific Types of ENSO, Journal of Climate 2009, **22**(3) 615-632.

17. Lorenzo, E. D., Schneider, N., Cobb, K.M., Franks,P.J.S., Chhak, K., Miller, A.J. McWilliams, J.C., Bograd, S.J. Arango, H., Curchitser, E., Powell, T.M. and Riviere, P., North Pacific gyre oscillation links ocean and ecosystem change, Geophys Res. Letts 2008, **35** L08607 1-6.

18. VIRGO radiometer data, 2012, http://sohowww.nascom.nasa.gov/data/data.html

19. Engels, S. and van Geel, B., The effects of changing solar activity on climate: contributions from palaeoclimatological studies , J. Space Weather Space Clim. 2012, **2** A09 1-9 (2012).

20. Loehle, C. and McCullock, H. J., Correction to: A 2000 year global temperature reconstruction based on non-tree ring proxies, Energy and Environment, 2008, **19**(1) 93-100.

21. Barbante, C. et al, EPICA community members, (84 Authors), One to one coupling of glacial climate variability in Greenland and Antarctica, Nature, 2006, **444** 195-198.

22. Augustin, L. et al, EPICA community members, (56 Authors), Eight glacial cycles from an Antarctic ice core, Nature, 2004, **429** 623-627.

23. Tzedakis, P. C., Wolff, E.W., Skinner, L.C., Brovkin, V., Hodell, D.A., McManus, J.F. and Raynaud, D., Can we predict the duration of an interglacial? Climate of the Past 2012, **8** 1473-1485.

24. Rorsch, A., Should we change emphasis in greenhouse-effect research? Energy and Environment 2010, **21**(4) 165-170

25. A. A. Tsonis, An Introduction to Atmospheric Thermodynamics, 2nd edn., Cambridge University Press, Cambridge, UK, 2007.

26. IEEE Standard for calculating the current temperature relationship of bare overhead conductors IEEE Standard 738, 1993.

27. Yu, L., Jin, X. and Weller R. A., Multidecade Global Flux Datasets from the Objectively Analyzed Air-sea Fluxes (OAFlux) Project: Latent and Sensible Heat Fluxes, Ocean

Evaporation, and Related Surface Meteorological Variables, OAFlux Project Technical Report (OA-2008-01) Jan 2008.

28. Yu, L., Global variations in oceanic evaporation (1958-2005): The role of the changing wind speed, J. Climate, 2007, **20**(21) 5376-5390.

29. Yu, L.and R. A. Weller, Objectively Analyzed air-sea heat Fluxes (OAFlux) for the global oceans, Bull. Amer. Meteor. Soc., 2007, **88**, 527-539,

30. Yu, L., 2012, http://oaflux.whoi.edu/images2_flux/EV_50a.jpg

31. Mengelcamp H.T., et al., (25 Authors), Evaporation over a heterogenous land surface, Bull. Amer. Met. Soc. 2006, **87**(6) 775-786

32. Billo E.J., Excel for Scientists and Engineers, J. Wiley & Sons, Hoboken, NJ, 2007

33. Goulden, M. L., Ameriflux Data, Grasslands Site, 2012,

http://ameriflux.ornl.gov/fullsiteinfo.php?sid=193

34. Eschenbach, W., The thunderstorm thermostat hypothesis, Energy and Environment, 2010, **21**(4) 201-200.

35. NASA, U. S. Standard Atmosphere, NASA-TM-X-74335, 1976.

36. Lacis, A. A. and Oindas, V., A description of the correlated k distributing method for modeling non gray gaseous absorption, thermal emission and multiple scattering in vertically inhomogenous atmospheres, J. Geographical Res., 1991, **96**(D5) 9027-9063,

37. Rothman, L.S. et al, (30 authors), The HITRAN 2004 molecular spectroscopic database, J. Quant. Spectrosc. Rad. Trans., 2005, **96** 139-204.

38. Feldman D.R., Liou K.N., Shia R.L. and Yung Y.L., On the information content of the thermal IR cooling rate profile from satellite instrument measurements, J. Geophys Res. 2008, 113 D1118 pp1-14.

39. Seidel, D. J., Free, M., and Wang, J.., Diurnal cycle of upper air temperature estimated from radiosondes, J. Geophys Res. 2005, **110** D090102 1-13

40. Hale, G. M. and Querry, M. R., Optical constants of water in the 200 nm to 200 µm region Applied Optics, 1973, **12** 555-563.

41. Hansen, J. et al, (45 authors), Efficacy of climate forcings, J. Geophys. Research, 2005, **110** D18104 pp1-45.

42. Alexander, M. A., Timlin, M.S., and Scott, J.D., Winter to winter recurrence of sea surface temperature, salinity and mixed layer depth anomalies Progress in Oceanography 2001, **49** 41-61

43. D'Aleo, J., 'Effects of AMO and PDO on temperatures', Intellicast, May 2008, http://www.intellicast.com/Community/Content.aspx?a=127